03.5

Statistical analysis of Taylor bubble formation in a capillary pipe

© F.V. Ronshin[1,2], D.Y. Kochkin[1,2], Y.A. Dementyev[1,2], K.S. Eloyan[1,2], I.S. Vozhakov[1,2]

[1] Novosibirsk State University, Novosibirsk, Russia
[2] Kutateladze Institute of Thermophysics, Siberian Branch, Russian Academy of Sciences, Novosibirsk, Russia
E-mail: f.ronshin@gmail.com

Received December 10, 2021
Revised January 10, 2022
Accepted January 11, 2022

An experimental study of the Taylor regime in a pipe with an inner diameter of 2 mm has been carried out. A method for studying the Taylor regime in a capillary pipe using automatic image analysis to measure the main characteristics of bubbles has been developed and applied for the first time. The dependences of the gas bubble and liquid slug lengths on the gas and liquid velocities are studied. It was found that in the region of the stable Taylor regime, the standard deviation of the bubble sizes is close to the accuracy of the research method. The dispersion of the bubble size distribution increases near the regime boundary. It is shown that, based on the statistical analysis of a large amount of data, it can be concluded that there is a coalescence and fragmentation of bubbles.

Keywords: capillary pipe, two-phase flow, Taylor regime, statistical analysis.

DOI: 10.21883/TPL.2022.03.52892.19105

During the last two decades, the use of microreactors became one of the important methods for intensifying processes in chemical and processing industries [1] due to the heat and mass transfer efficiency that is at present important for the chemical production. The potential of using microreactors was demonstrated in many applications like mixing [2], separation [3], reactions [4] and chemical analysis [5]. In mini−channels, the piston flow regime, or the Taylor flow regime, is one of the main flow modes taking place in a wide range of gas and liquid flow rates [6]. In the Taylor regime, the flow consists of long bubbles separated by liquid slugs. The Taylor bubbles are enveloped with thin liquid films and have lengths exceeding the channel effective diameter. Fundamental data on this flow regime have been obtained for channels of different geometry. In some cases, information on the regime stability is also needed. In the pharmaceutical industry, Taylor bubbles are used to obtain small medicine doses, while in the chemical industry they are used in high−precision certain−ratio mixing, nanoparticle synthesis [7], and in catalyzed gas−liquid reactions [8]. In such cases, the bubble size deviations should be predictable and controllable. In this study, the statistical analysis of the Taylor bubble lengths was performed based on a great amount of experimental data by using the automatic algorithm.

For the Taylor regime investigation, an operating bench was developed and assembled (Fig. 1). For visualization, a glass pipe 2 mm in inner diameter and 12 cm in length was used. The liquid (water Milli-Q®) was supplied using a syringe liquid pump Cole-Parmer®; the gas (nitrogen) was fed from the cylinder, its flow rate was set by flow rate controller Bronkhorst®. The flow meter signal processing, as well as the gas flow rate control, was performed using the National Instruments® analog−digital converter. The operating fluid purity was controlled by measuring the liquid surface tension with tensiometer KRUSS K100. The two−phase flow in the pipe was visualized with a high−speed camera Vision Research Phantom® v.7.0 with the framerate of 1000 fps. The camera covered the pipe section 29 mm long with the spatial resolution of 40 px/mm. The superficial gas velocity U_{SG} defined as the gas flow rate divided by the pipe cross section was 0.1 to 0.6 m/s, that of liquid (U_{SL}) was 0.05 to 0.3 m/s.

For processing the data acquired by visualization of bubbles in the Taylor flow regime, and for obtaining necessary quantitative characteristics, a Matlab® algorithm was developed. The automatic image analysis technique gave a good account of itself in processing images in mini— and micro-systems [9], as well as in studying the dynamics of the bubble growth in boiling [10]. To the program code input, images recorded in the experiment by high−speed camera Phantom® are fed. Then the images are analyzed, and regions corresponding to gas bubbles and liquid slugs are determined. After that, analysis of the bubbles is performed (their positions, sizes and other parameters are determined). The same analysis is performed for the next frame. Thus, time evolution of each bubble is analyzed, which enables determination of the bubble velocities. Finally, data on size and velocity are fixed for each bubble. The same analysis is performed for liquid slugs. The measurement accuracy is governed by the ambiguity of determining the gas−liquid phase interface that is 1 px or 0.025 mm.

Fig. 1 presents a typical processed image. Each bubble is numbered, and the program monitors their evolution in time. For each bubble, its length and the liquid slug length are also given. For each gas and liquid flow rate, 3000 frames have been analyzed. For each frame, the program records in a file the bubble sizes, velocities and liquid slug lengths, etc.

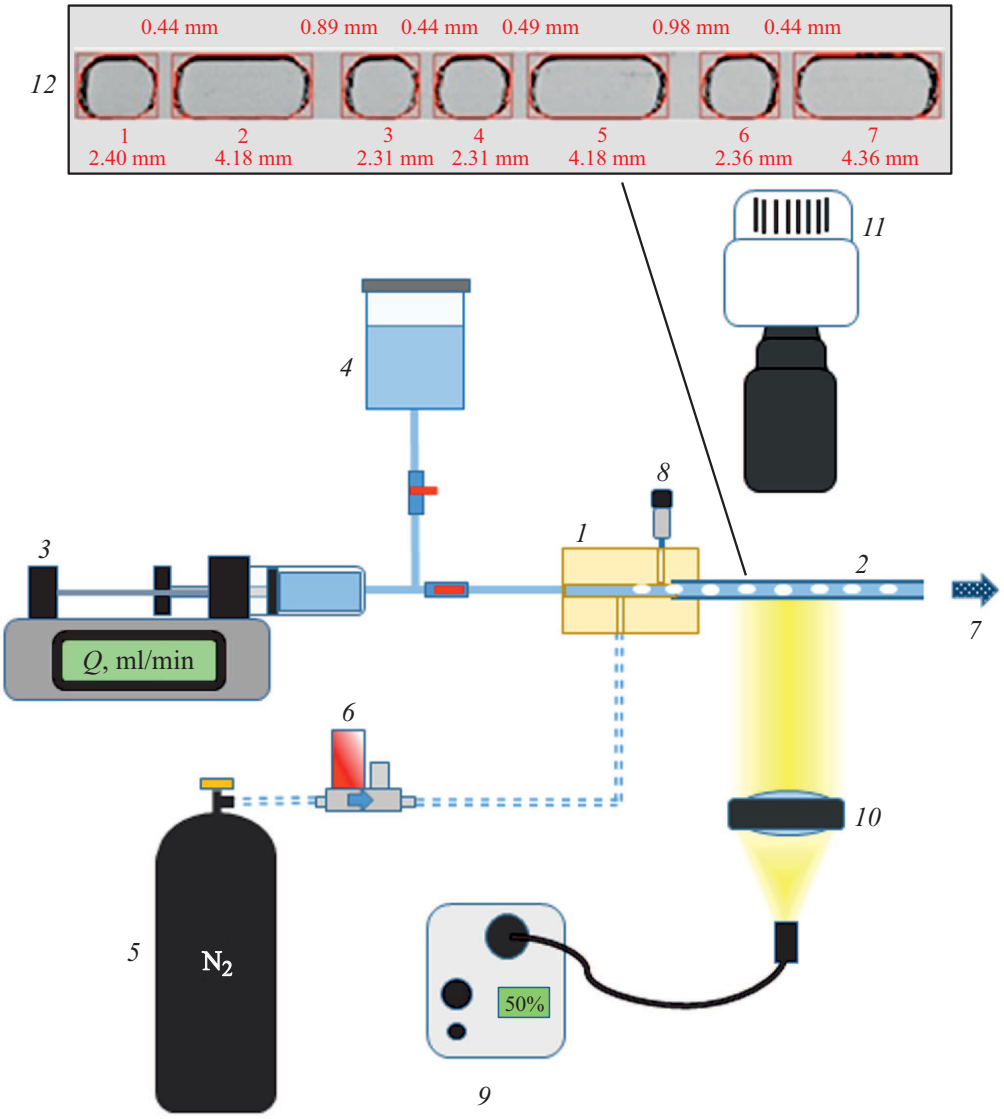

Figure 1. Experimental bench for studying the two−phase flow in a circular channel and a case of data processing with the developed algorithm. *1* — T-joint, *2* — operating section, *3* — syringe fluid pump, *4* — water tank Milli-Q, *5* — nitrogen cylinder, *6* — flow rate controller, *7* — vent to the atmosphere, *8* — pressure gauge, *9* — light source, *10* — lens, *11* — high−speed camera, *12* — image processed with the automatic algorithm.

Fig. 2 presents the bubble length distribution depending on the superficial gas and liquid velocities. At low superficial velocities of liquid and gas ($U_{SL} = 0.1$ m/s, $U_{SG} = 0.1$ m/s), the bubble lengths differ insignificantly. For instance, the mean bubble length $\langle L_b \rangle$ is 1.92 mm, while the standard deviation σ is 0.03 mm and is comparable with the measurement accuracy (at the sampling size of 2674 bubbles). When the superficial liquid velocity increases to $U_{SL} = 0.2$ m/s, the mean bubble size decreases to 1.52 mm, while the standard deviation remains invariant (at the sampling size of 364 bubbles). When the superficial gas velocity increases to $U_{SG} = 0.2$ m/s ($U_{SL} = 0.1$ m/s), the mean length $\langle L_b \rangle$ increases to 2.61 mm, while standard deviation σ increases by 2.5 times to 0.07 mm (at the sampling size of 210 bubbles). Further increase in the gas velocity ($U_{SG} = 0.3$ m/s) and approaching the Taylor regime boundaries gives rise to the bubble coalescence. In this case, the bubbles in the channel (about 90% of all the bubbles) exhibit a certain characteristic size and also sizes multiple to the characteristic one because of the coalescence of several bubbles. In this case, more informative is not mean length $\langle L_b \rangle = 4.02$ mm, but median length $L_b = 3.64$ mm. In the presence of coalescence, the standard deviation increases to 1.18 mm (at the sampling size of 178 bubbles), however, this value appears to be 0.13 mm if bubbles formed by coalescence are excluded.

With further increase in the gas velocity, transient regimes are observed: fractions of coalescing and primary bubbles become comparable, the probability of the cascade coalescence increases significantly, and sizes of the observed

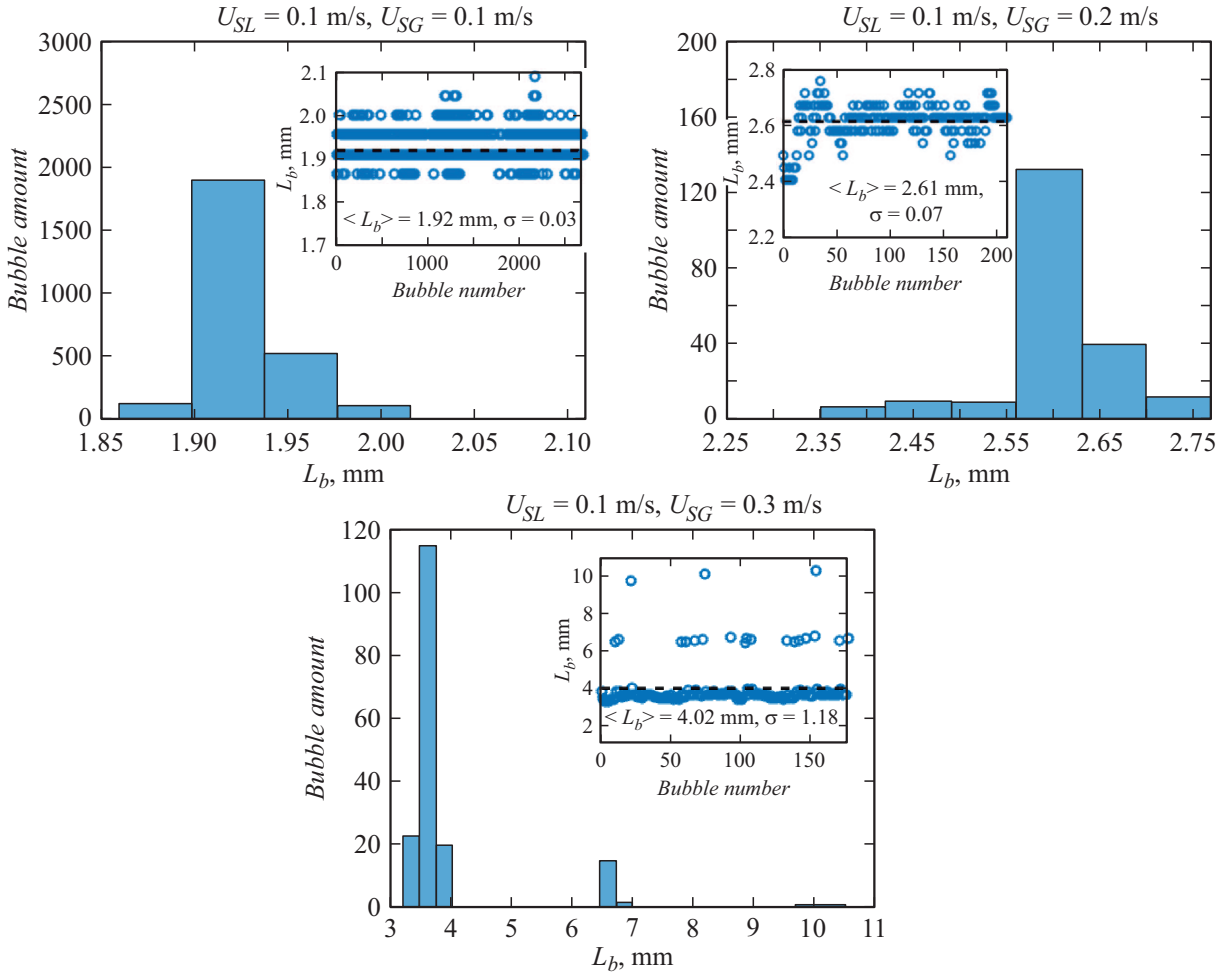

Figure 2. Bubble length distributions depending on the reduced gas and liquid velocities.

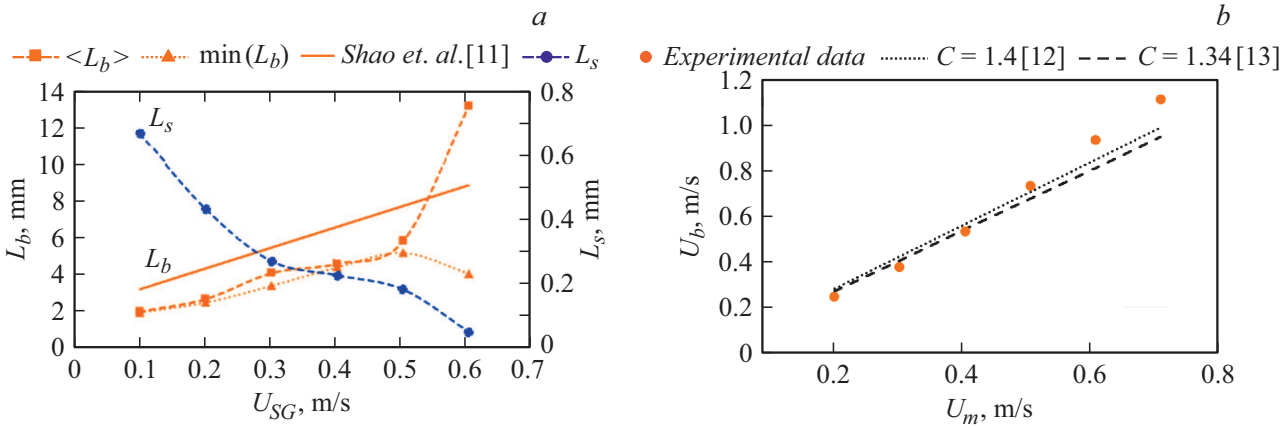

Figure 3. *a* — gas bubble and liquid slug lengths versus superficial gas velocity at $U_{SL} = 0.1$ m/s. *b* — gas bubble velocity versus the mixture velocity at $U_{SL} = 0.1$ m/s.

bubbles may differ by 10 times. The minimal bubble sizes for different gas velocities U_{SG} are shown in Fig. 3, *a*. A gradual rise in the minimal bubble size is observed in the velocity range of 0.1–0.5 m/s, and a sharp drop takes place at 0.6 m/s. Evidently, the decrease in the minimal size is connected with fragmentation of long bubbles that have been formed due to the cascade coalescence.

Fig. 3, *a* presents the dependence of lengths of gas bubbles L_b and liquid slugs L_s on the superficial gas velocity U_{SG}. It is clearly seen that the bubble size increases with

increasing superficial gas velocity. The increase retains its gradual character up to the gas velocity of 0.5 m/s. As a result of the coalescence, multiple–size bubbles are periodically observed, but they do not significantly contribute to the flow structure. A sharper increase in the mean bubble size takes place at higher superficial gas velocities. This is caused by a considerable increase in the coalescence probability, which is confirmed by the analysis of the bubble length distribution. In the figure, the solid line represents the correlation [11]: $L_b = (1 + 0.57U_{SG}/U_{SL})D$. Experimental data lie somewhat lower than the presented dependence. Only one point is unsettled, just that where the coalescence significantly affects the bubble size distribution.

Fig. 3, *b* presents the bubble velocity dependence on the mixture velocity U_m defined as a sum of the superficial gas and liquid velocities. One can see that the bubble size monotonically increases with increasing superficial gas velocity. The effect of parameters of the interphase distribution in the flow is governed by the distribution parameter C. The bubble velocity in horizontal pipes is defined as product $U_b = CU_m$. Fig. 3, *b* clearly demonstrates the agreement between the experimental data with correlations for $C = 1.4$ [12] and 1.34 [13].

In conclusion, we have developed and assembled an operating bench for studying the Taylor flow regime in a circular pipe 2 mm in diameter equipped with a T-joint. To process experimental data acquired from visualization and to obtain quantitative characteristics, there was developed and applied for the first time an algorithm analyzing time evolution of the bubbles and liquid slugs and also allowing determination of their sizes and velocities in the capillary pipe. It has been shown that bubble lengths at low superficial velocities of gas ($U_{SG} = 0.1$ m/s) and liquid ($U_{SL} = 0.1$ m/s) slightly differ from the mean value, while the standard deviation is comparable with the research method accuracy. The growth of liquid velocity does not lead to an increase in the absolute value of the bubble size spread but decreases their mean size. The increase in the superficial gas velocity results in a significant increase in the bubble size deviation from the mean value. For instance, the superficial gas velocity increase to $U_{SG} = 0.2$ m/s causes the 2.5 times increase in the standard deviation. When the gas velocity increases and gas approaches the Taylor regime boundaries, the bubble coalescence is observed. This results in arising of multiple peaks in the bubble size distribution and in a sharp (by an order of magnitude) growth of the standard deviation. Besides, in this case the mean bubble size differs considerably from the median value. For instance, at the gas velocity $U_{SG} = 0.3$ m/s and liquid velocity $U_{SL} = 0.1$ m/s these sizes differ by about 10%. If the gas velocity increases even more, a transient regime occurs in which no distinguishable bubble size is observed, while the minimal and maximal size may differ 10 times, which is due to both the cascade coalescence and fragmentation of bubbles.

Financial support

The study was supported by the Russian Scientific Foundation (project № 20-79-10096).

Conflict of interests

The authors declare that they have no conflict of interests.

References

[1] M.N. Kashid, L. Kiwi-Minsker, Ind. Eng. Chem. Res., **48**, 6465 (2009). DOI: 10.1021/ie8017912
[2] J. Hou, G. Qian, X. Zhou, Chem. Eng. J., **167**, 475 (2011). DOI: 10.1016/j.cej.2010.10.054
[3] N. Oozeki, S. Ookawara, K. Ogawa, P. Löb, V. Hessel, AlChE J., **55**, 24 (2009). DOI: 10.1002/aic.11650
[4] P. Lang, M. Hill, I. Krossing, P. Woias, Chem. Eng. J., **179**, 330 (2012). DOI: 10.1016/j.cej.2011.11.015
[5] E. Livak-Dahl, I. Sinn, M. Burns, Ann. Rev. Chem. Biomol. Eng., **2**, 325 (2011). DOI: 10.1146/annurev-chembioeng-061010-114215
[6] A.V. Minakov, A.A. Shebeleva, A.A. Yagodnitsyna, A.V. Kovalev, A.V. Bilsky, Tech. Phys. Lett., **43** (9), 857 (2017). DOI: 10.1134/S1063785017090231.
[7] A. Günther, S.A. Khan, M. Thalmann, F. Trachsel, K.F. Jensen, Lab Chip, Iss. 4, 278 (2004). DOI: 10.1039/B403982C
[8] T. Yasukawa, W. Ninomiya, K. Ooyachi, N. Aoki, K. Mae, Chem. Eng. J., **167**, 527 (2011). DOI: 10.1016/j.cej.2010.08.077
[9] F. Ronshin, Y. Dementyev, D. Kochkin, K. Eloyan, I. Vozhakov, Exp. Therm. Fluid Sci., **132**, 110565 (2022). DOI: 10.1016/j.expthermflusci.2021.110565
[10] V. Serdyukov, I. Malakhov, A. Surtaev, J. Visualization, **23**, 873 (2020). DOI: 10.1007/s12650-020-00660-z
[11] N. Shao, W. Salman, A. Gavriilidis, P. Angeli, Int. J. Heat Fluid Flow., **29**, 1603 (2008). DOI: 10.1016/j.ijheatfluidflow.2008.06.010
[12] D.J. Nicklin, Chem. Eng. Sci., **17**, 693 (1962). DOI: 10.1016/0009-2509(62)85027-1
[13] K. Mishima, T. Hibiki, H. Nishihara, Int. J. Multiphase Flow, **19**, 115 (1993). DOI: 10.1016/0301-9322(93)90027-R